Agricultural and Forest Meteorology 263 (2018) 373–387

Contents lists available at ScienceDirect

Agricultural and Forest Meteorology

journal homepage: www.elsevier.com/locate/agrformet

Climate change impact on Mexico wheat production

Ixchel M. Hernandez-Ochoa[a], Senthold Asseng[a,*], Belay T. Kassie[a,b], Wei Xiong[a,d], Ricky Robertson[c], Diego Notelo Luz Pequeno[d], Kai Sonder[d], Matthew Reynolds[d], Md Ali Babar[e], Anabel Molero Milan[d], Gerrit Hoogenboom[f]

[a] Department of Agricultural and Biological Sciences, University of Florida, FL 32611, USA
[b] DuPont Pioneer, 8650 NW 62nd Avenue, Johnston, IA, 50131, USA
[c] International Food Policy Research Institute, Washington, DC, 20006-1002, USA
[d] International Maize and Wheat Improvement Center, Apdo. Postal 6-641, 06600, D.F, Mexico
[e] Department of Agronomy, University of Florida, FL, 110965, USA
[f] Institute for Sustainable Food Systems, Frazier Rogers Hall, University of Florida, Gainesville, FL, 32611, USA

ARTICLE INFO

Keywords:
Triticum
Model ensemble
Crop simulation model
Uncertainty

ABSTRACT

Wheat is one of the most important cereal crops in Mexico, but the impact of future climate change on production is not known. To quantify the impact of future climate change together with its uncertainty, two wheat crop models were executed in parallel, using two scaling methods, five Global Climate Models (GCMs) and two main Representative Concentration Pathways (RCPs) for the 2050s. Simulated outputs varied among crop models, scaling methods, GCMs, and RCPs; however, they all projected a general decline in wheat yields by the 2050s. Despite the growth-stimulating effect of elevated CO_2 concentrations, consistent yield declines were simulated across most of the main wheat growing regions of Mexico due to the projected increase in temperature. Exceptions occurred in some cooler areas, where temperature improved sub-optimal conditions, and in a few areas where rainfall increased, but these increases only provided negligible contributions to national production. Larger and more variable yield declines were projected for rainfed wheat due to current and projected spatial variability of temperature and rainfall patterns. Rainfed wheat, however, only contributes about 6% of Mexico's wheat production. When aggregating the simulated climate change impacts, considering temperature increase, rainfall change, and elevated atmospheric CO_2 concentrations for irrigated and rainfed wheat cropping systems, national wheat production for Mexico is projected to decline between 6.9% for RCP 4.5 and 7.9% for RCP 8.5. Model uncertainty (combined for crop and climate models) in simulated yield changes, and across two scaling methods, was smaller than temporal and spatial variability in both RCPs. Spatial variability tends to be the largest in both future scenarios. To maintain or increase future wheat production in Mexico, adaptation strategies, particularly to increasing temperatures affecting irrigated wheat, or expanding the cropping area, will be necessary.

1. Introduction

Wheat is one of the major cereal crops in the world because of its importance as a main source of energy and protein in human diets (Curtis et al., 2002). In Mexico, wheat is among the top five produced crops: national production during the 2015–2016 season was 3.8 million tons (around $750 million value), cultivated on 720,000 ha (SAGARPA, 2016b). Production is concentrated in Sonora, Baja California, Sinaloa, Guanajuato, and Michoacán states, which together represent about 86% of the total national production (SAGARPA, 2016a). More than 90% of the produced wheat is irrigated due to the arid and semi-arid climate in most of the wheat production area. Rainfed wheat production is typical of the high elevation areas in the central and southern states and Mediterranean-type climate in Baja California, where winter and spring temperature and rainfall are more suitable for the cropping system (Escobar, 2014).

Past global temperature trends already show the effects of warming temperatures on wheat production. Historical wheat yield analysis showed a 5.5% global decline in aggregated wheat production since 1980, as a result of increased global mean temperature (Lobell et al., 2011). In Mexico, Asseng et al. (2014) reported warming decadal trends in Obregon (Sonora) and Toluca (Mexico State) of 0.46 and 0.27 °C,

* Corresponding author. Current address: Department of Agricultural and Biological Sciences, University of Florida, FL 32611, USA.
E-mail address: sasseng@ufl.edu (S. Asseng).

https://doi.org/10.1016/j.agrformet.2018.09.008
Received 16 March 2018; Received in revised form 7 September 2018; Accepted 10 September 2018
Available online 17 September 2018
0168-1923/ © 2018 Elsevier B.V. All rights reserved.

respectively, which have caused wheat yield declines from 2 to 3% per decade for the period from 1980 to 2010. However, Lobell et al. (2005) reported that wheat yields in Northwest Mexico have increased by 25% from 1980 to 2001, mostly due to cooling trends in night minimum temperature likely causing reduced plant respiration.

Global temperature trends in the future suggest continuous warming by up to 2 °C at mid-century (IPCC, 2013), which may result in further wheat yield decline if no adaptation strategies are applied (Asseng et al., 2014; Challinor et al., 2014). Elevated atmospheric CO_2 in the future can have a positive effect on crop growth and yields but its response is limited to temperature, nitrogen (N), and water conditions (Alexandrov and Hoogenboom, 2000; Kimball et al., 2001). Climate change projections for Mexico differ in severity, but all of them report a warmer and drier climate by mid-century (Conde et al., 2011; Karmalkar et al., 2011; Peterson et al., 2002; SAGARPA and FAO, 2012), increasing the concern over how climate change will further affect wheat production. Few studies on the effects of climate change on Mexico's wheat production were conducted in the past. SAGARPA and FAO (2012) conducted a study to determine the effects of climate change on Mexican wheat production by using one General Climate Model (GCM). Results showed average yield declines in the Northwest by up to 75%, but also projected 50% yield increases in Baja California and North Sonora. Another study conducted by Parry et al. (2004) also using one GCM with multiple emission scenarios and yield transfer functions, projected a 5–10% yield decline in national production, even when considering adaptation strategies. The use of one GCM and one method to estimate impact yields limits these studies and increases uncertainty, as climate and crop model responses tend to vary widely (Giorgi and Francisco, 2000). In addition, the use of many GCMs is a common practice nowadays when conducting climate change assessments (Semenov and Stratonovitch, 2010).

Climate and crop simulation models contain errors due to their structure and parameterization, which cause uncertainty in projections (Asseng et al., 2013a; Tebaldi and Knutti, 2007). This uncertainty can be quantified through the use of multi-model ensembles (Asseng et al., 2013a; Martre et al., 2015; Wallach et al., 2016). Using the median or mean of multi-model ensembles has proven to be closer to observations than a single model in a diverse range of crops and environments (Asseng et al., 2013a; Martre et al., 2015; Palosuo et al., 2011; Rotter et al., 2012; Yin et al., 2017). The use of multi-model ensembles and different simulation methods provides a better understanding of the range of future climate change impacts on crop production and gives more confidence for building adaptation strategies for future decades (Asseng et al., 2013a; Dale et al., 2017). The main goal of this study was to explore the future impacts of climate change and its uncertainty on Mexican wheat production by using multiple climate and crop model and two scaling approaches.

2. Materials and methods

2.1. Simulation methods

The study was conducted using point and spatial simulation methods. Observed five year average (2010–2014) production and yield levels for wheat in Mexico (SAGARPA, 2016a) were used to select 32 reference locations for the point simulation method. Locations were selected capturing the diverse yield levels and environmental conditions for irrigated and rainfed wheat (Table 1, Fig. 1). Most reference locations are within the Northwestern states, where the majority of wheat production occurs. Major environmental characteristics for reference locations are provided in Table 1. An additional spatial simulation method was also conducted by using the MINK system, which is a is a global-scale gridded simulation platform (Robertson, 2017), using the same crop and climate models from the point simulations. Simulations were performed using 0.5° resolution considering the 2015 wheat production areas (SAGARPA, 2016a). Crop simulation models, input data for climate, crop management, soil profiles, planting dates, and cultivar selection and distribution were the same for both simulation methods.

2.2. Crop model selection and inputs

2.2.1. Crop simulation models

The CROPSIM and NWheat crop simulation models embedded within the platform of the Decision Support Systems for Agrotechnology Transfer, DSSAT v4.6 (Jones et al., 2003) were selected to conduct the study. Both models simulate the crop's life cycle based on Zadok's scheme (Asseng et al., 2013b; Hunt and Pararajasingham, 1995; Zadoks et al., 1974). CROPSIM temperature responses are structured in cardinal temperature functions that control crop growth and development, and organic matter mineralization (Hunt and Pararajasingham, 1995). The NWheat model was derived from ASPSIM-NWheat (Asseng, 2004; Asseng et al., 1998, 2004; Kassie et al., 2016). Temperature in NWheat affects phenology, biomass accumulation, CO_2 assimilation, leaf senescence during grain filling, rate of grain filling, and N demand to grain and vapor pressure deficit (Zheng et al., 2015). Both models run on a daily time step using the radiation use efficiency approach for crop biomass accumulation, and have been widely used to study cropping systems under different environments (Asseng et al., 2004; Asseng and Turner, 2007; Asseng et al., 2002, 2000; Lazzaretti et al., 2015; Ruane et al., 2016; van Bussel et al., 2016; Van Ittersum et al., 2003).

2.2.2. Observed data

Observed annual wheat yield, production, and planted area at state and district level for the baseline period (1980–2010) were collected from SAGARPA (2016a) to compare with the simulated wheat yields. Grain yield data was corrected to 0% moisture. In addition, wheat yields showed a positive linear trend through the baseline period, likely due to improvement in cultivar genetics and cultural practices. Therefore, wheat yields were detrended by using the following formula:

Adjusted yield = y + m*(LY-CY)

Where:

y = yield for the current year
m = slope from the linear regression in baseline wheat yield
LY = last year from the baseline period
CY = current year to be adjusted

Phenology and yield related variables from a 6-year experiment conducted in Obregon, Sonora (Sayre et al., 1997) were collected to compare phenology and yield variables with the simulated data.

2.2.3. Climate data

The years 1980 to 2010 were selected as the historical baseline to compare with future climate change impacts on wheat production. This climate period was selected following the procedures of the Agricultural Model Intercomparison and Improvement Project (AgMIP) and it is considered a sufficient period to allow climatological analysis (Guttman, 1989; Rosenzweig et al., 2013; WMO, 1989). Climate data for the reference locations were collected from available gridded climate datasets within the MINK system (Robertson, 2017). The baseline and future climate data for each reference location were extracted from the grid cell where the reference point coordinates were located (Table 1). Daily maximum (T_{max}) and minimum (T_{min}) temperature, rainfall, and solar radiation in the MINK system were collected from National Centers for Environmental Prediction and University Corporation for Atmospheric Research (NCEP/NCAR) reanalysis database (Kalnay et al., 1996). The spatial resolution of the NCEP data for T_{max} and T_{min} was about 1.884 °N/S and 1.865 °E/W. Rainfall data at 0.5° resolution corresponding to the same time period was collected from the Global Precipitation Climatological Center of the National Oceanic

Table 1
Locations representing wheat-growing areas in Mexico.

#	State	Coordinates		Soil characteristics			Mega Environment	Cultivar type[d]	Winter[a]		Summer[b]	
		Latitude	Longitude	Texture	Fertility[c]	Depth			Tmean (°C)	Rainfall (mm)	Tmean (°C)	Rainfall (mm)
1	Sonora	32.25	−114.75	Loam	High	Medium	4A, 4B, 4C	Spring	13.6	26	27.5	12
2	Baja California	31.75	−116.25	Loam	High	Shallow	4A, 4B, 4C	Spring	13.7	200	24.0	14
3	Chihuahua	31.25	−108.25	Loam	Low	Medium	12	Winter[e]	8.7	52	23.6	171
4	Sonora	30.75	−112.75	Loam	High	Medium	4A, 4B, 4C	Spring	13.2	49	28.8	75
5	Chihuahua	30.75	−106.75	Loam	Low	Medium	12	Winter	8.5	40	22.5	205
6	Sonora	30.25	−111.25	Loam	High	Medium	4A, 4B, 4C	Spring	14.1	64	28.5	205
7	Baja California	29.25	−114.25	Loam	Low	Medium	4A, 4B, 4C	Spring	15.4	60	27.1	18
8	Sonora	29.25	−111.25	Loam	Low	Medium	4A, 4B, 4C	Spring	14.1	50	28.5	209
9	Coahuila	29.25	−102.25	Loam	High	Shallow	4A, 4B, 4C	Spring	12.6	51	24.6	139
10	Chihuahua	28.75	−106.25	Loam	Low	Medium	2A, 2B	Spring	9.4	33	21.6	307
11	Chihuahua	28.25	−104.25	Clay	Low	Shallow	4A, 4B, 4C	Spring	10.4	32	19.3	245
12	Coahuila	28.25	−101.75	Loam	High	Shallow	4A, 4B, 4C	Spring	15.1	65	25.5	198
13	Coahuila	28.25	−101.25	Loam	High	Shallow	1	Spring	15.1	67	25.5	208
14	Sonora	28.25	−109.25	Loam	High	Shallow	2A, 2B	Spring	13.7	110	24.9	468
15	Sonora	27.75	−110.25	Loam	High	Shallow	1	Spring	16.7	55	28.7	195
16	Coahuila	27.75	−103.25	Loam	Low	Medium	4A, 4B, 4C	Spring	13.0	37	22.2	150
17	Chihuahua	27.75	−108.25	Loam	High	Shallow	2A, 2B	Spring	13.7	116	24.9	558
18	Sinaloa	26.25	−108.25	Clay	High	Medium	1	Spring	17.7	87	25.8	566
19	Baja California Sur	25.25	−111.25	Loam	High	Medium	4A, 4B, 4C	Spring	19.1	36	27.5	153
20	Coahuila	25.25	−101.75	Loam	High	Shallow	4A, 4B, 4C	Spring	14.9	36	22.1	221
21	Durango	25.25	−106.25	Clay	High	Medium	2A, 2B	Spring	14.2	133	21.3	705
22	Nuevo Leon	25.25	−98.75	Clay	High	Medium	4A, 4B, 4C	Spring	17.8	86	25.5	325
23	Nuevo Leon	24.25	−100.25	Loam	High	Shallow	4A, 4B, 4C	Spring	18.0	61	22.7	212
24	Durango	24.25	−104.75	Clay	High	Medium	4A, 4B, 4C	Spring	15.2	40	19.6	350
25	Zacatecas	24.25	−102.25	Loam	High	Shallow	4A, 4B, 4C	Spring	12.6	27	16.8	189
26	Zacatecas	23.75	−103.25	Loam	High	Deep	4A, 4B, 4C	Spring	12.6	27	16.8	276
27	Michoacán	20.25	−100.25	Clay	High	Medium	2A, 2B	Spring	13.8	38	16.3	459
28	Hidalgo	20.25	−99.25	Clay	High	Medium	2A, 2B	Spring	13.8	32	16.3	234
29	Michoacán	19.75	−101.25	Loam	High	Medium	2A, 2B	Spring	14.9	42	16.4	539
30	Puebla	18.25	−97.25	Sand	Low	Medium	2A, 2B	Spring	16.0	92	19.0	681
31	Oaxaca	17.25	−96.75	Clay	High	Medium	2A, 2B	Spring	16.0	94	19.0	692
32	Chiapas	15.25	−92.25	Loam	High	Medium	1	Spring	22.3	57	22.4	1111

[a] Winter season period from December 10 to March 30 for the baseline (1980–2010).
[b] Summer season from July 1 to Sept 7 for the baseline (1980–2010).
[c] Soil organic matter content of top soil (SOC, %): High: SOC ≥ 1.2; Medium: 0.7 ≤ SOC < 1.2; Low: 0.0 ≤ SOC < 0.7.
[d] Cultivar distribution and selection from Gbegbelegbe et al. (2017).
[e] Winter cultivars corresponding to cold dessert climate, high elevation areas, according to Köppen Climate Classification System (Kottek et al., 2006).

and Atmospheric Administration (GPCC NOAA, US).

For the future scenarios, Representative Concentration Pathways (RCPs) 4.5 and 8.5 were selected for mid-century (2050s) impact assessment. The RCPs are greenhouse gas concentration trajectories for future climate adopted by the Intergovernmental Panel on Climate Change (IPCC, 2013). Five downscaled and bias-corrected GCM scenarios (Table 2) from the Inter-Sectoral Impact Model Intercomparison Project (ISI-MIP, revised version from November 2015) were collected

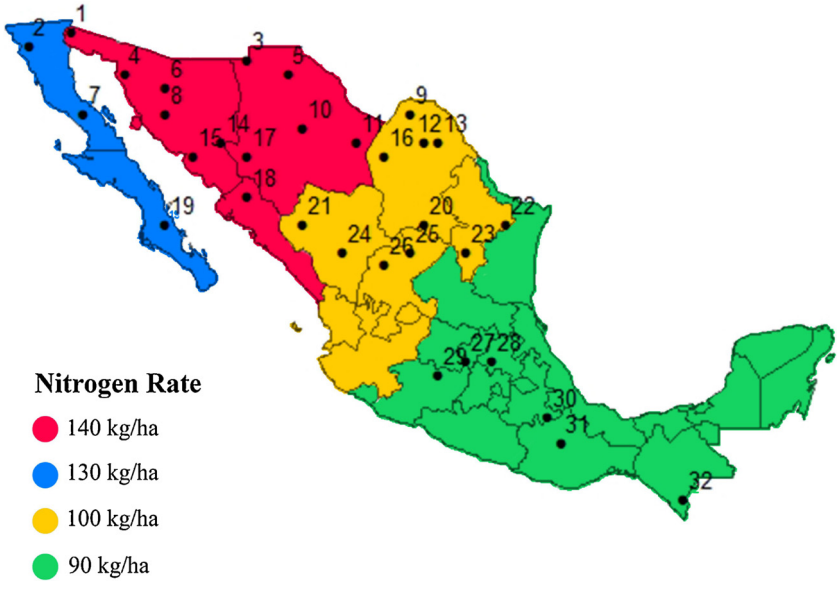

Fig. 1. Applied N - fertilizer amounts for irrigated wheat and distribution of the 32 reference locations in Mexico.

Table 2
Global Climate Models for climate scenario simulations provided daily data on maximum and minimum temperature, rainfall, and solar radiation.

Climate model	Model acronym
Geophysical Fluid Dynamics Laboratory-Earth System Model	GFDL-ESM2M
Institute Pierre Simon Laplace- Coupled Model	IPSL-CM5A-LR
Hadley Centre Global Environment Earth System Model	HadGEM2-ES
Model for Interdisciplinary Research on Climate – Earth System Model	MIROC-ESM-CHEM
The Norwegian Earth System Model	NorESM1-M

from the Potsdam Climate Institute (Mueller and Robertson, 2014). Daily temperature and rainfall values were extracted and averaged into monthly averages for the baseline period (1980 to 2010) and the 2050s future period (2041–2070). Calculated monthly changes were applied to the daily climate of the historical weather data (baseline) to create future scenarios. The resulting daily value of temperature is the old daily value plus the calculated change between the future monthly value from the GCMs and the historical monthly value; daily rainfall values were handled using the same procedure. Solar radiation remained unchanged for the future scenarios.

2.2.4. Atmospheric CO_2

The atmospheric CO_2 level for the historical baseline (baseline level) was set to 362 ppm, corresponding to the 30-year mean of the baseline period (1980–2010). Crop simulations for future scenarios were conducted with the projected elevated atmospheric CO_2 to determine the combined effect of temperature, rainfall, and elevated CO_2. The atmospheric CO_2 levels for future scenarios (RCP 4.5 = 498 ppm, RCP 8.5 = 572 ppm) were based on the IPCC's latest report (IPCC, 2013). Additionally, crop simulations for the future scenarios were conducted using the baseline level of atmospheric CO_2 to estimate the effects of elevated atmospheric CO_2 on wheat yield.

2.2.5. Soil data and initial conditions

Soil characteristics for each location are described in the Table 1. The soil information corresponds to the geo-referenced HC27 generic soil profile database at 0.083° resolution created by Koo and Dimes (2010). The HC27 global soil distribution map was derived from the combination of three major texture types (clay, loam, sand), organic carbon levels (high, medium, low), and depths (shallow, medium, deep). Most of the soils in the reference locations for Mexico are within the category of loamy and clay soils, with variable organic carbon content and depth (Table 1). Initial surface residue was set to 3000 kg ha^{-1}, initial root mass was set to 1000 kg ha^{-1}, and initial mineral soil nitrogen (N) was set to 25 kg ha^{-1} (Gbegbelegbe et al., 2017). To ensure germination, and due to lack of initial water content observations, initial water content in the point simulations was set to 100% field capacity (FC) in the first 30 cm of the soil profile and at 10% FC for the rest of the soil profile. Point simulations were initialized one day before planting every year.

2.2.6. Crop management

Sowing dates were selected using observed data (Sayre et al., 1997) and expert knowledge. Selected sowing dates were December 10th for the winter and July 1st for the summer season. All irrigated wheat simulations were sown in winter, and most rainfed wheat simulations were sown in summer, except for in the Northwest (Baja California, Baja California Sur, Sonora, Chihuahua, and Sinaloa), where winter sowing was more suitable in terms of temperature and rainfall. Plant density was 300 plants per m^{-2} at a 5 cm planting depth. Initially, N fertilizer applications were based on Ramirez-Rodrigues et al., (2016) and Sayre et al., (1997), but adjusted to observed state wheat yield levels from SAGARPA (2016a). The N fertilizer rates for the irrigated wheat point simulations ranged from 90 to 140 kg ha^{-1}, and are presented in Fig. 1. For the gridded simulations, the N fertilizer distribution was divided by states, using the same amount as the reference point located in a particular state. The N application rate for rainfed wheat in all reference locations and in spatial simulations was 10 kg ha^{-1}, following the recommendations from Limon-Ortega and Villaseñor-Mir (2006). N fertilizer in irrigated wheat was split equally in two applications: one at sowing and the other at 40 days after sowing. In the case of rainfed wheat, a single application was performed at sowing. The fertilizer was applied as urea-N banded beneath the surface and incorporated at 5 cm. Water management for the irrigated treatment was set to automatic irrigation at 80% of maximum water available in the first 30 cm of the soil profile to reduce the risk of crop water stress.

2.2.7. Cultivar selection, distribution, and genetic coefficients

Cultivar selection was site-specific (Table 1). Wheat cultivars were selected according to the mega-environment distribution designed by CIMMYT, which assigns a cultivar type (spring, facultative, or winter) depending on growing conditions and disease pressures (Monfreda et al., 2008). Cultivar genetic coefficients from the CERES-Wheat simulation model were first extracted from Gbegbelegbe et al., (2017). The genetic coefficients were revised based on observed phenology and yields from the Obregon, Sonora experiment and state yield data from major production areas (SAGARPA, 2016a; Sayre et al., 1997). Revised coefficients were then adapted to CROPSIM and NWheat, matching the coefficients across the models depending on their definition and units. The updated set of cultivar genetic coefficients relevant for Mexico are shown in Table 3. Most of the selected cultivars were spring wheat types, commonly used across Mexico, with the exception of the cooler North Chihuahua high-elevation area, which falls into the winter type category.

2.3. Quantification of model performance

The NWheat model was previously tested with detailed field experiment data from Obregon, Sonora (Asseng et al., 2004), which is one of the most important wheat producing areas in Mexico. In addition, observed state level yield data for the baseline (1980–2010) (SAGARPA, 2016a) from major production areas in Sonora, Baja California, Guanajuato, Nuevo Leon, and Zacatecas were selected to compare simulated vs observed yields. Crop model performance was quantified by calculating the root mean square error per location over the 30-year baseline period for irrigated and rainfed wheat production. Correlation coefficients for combined irrigated and rainfed wheat yields at 95% confidence interval for the baseline period for the three major producing states were calculated from observations vs the simulated wheat yields. Individual correlation coefficients by state were also calculated.

2.4. Procedure to upscale the climate change impacts to observed wheat yields

Observed district irrigated and rainfed 2015 wheat production statistics in Mexico from SAGARPA (2016a) were used for the procedure. Each of the 32 simulated locations were assigned to a district and its wheat production, depending on proximity and yield level. Delta changes for each location were calculated by finding the percentage change of the RCP output versus the baseline period. Delta changes were then applied to the observed 2015 district wheat production. Future irrigated and rainfed wheat production were summed up to report an aggregated national production for the 2050s future period. For the spatial simulation method,

raster files corresponding to each mega-environment cultivar, nitrogen level, sowing dates, GCMs, and crop models were combined in one single national raster for each RCP, keeping separated irrigated and rainfed simulations. Then, the baseline and future national wheat production was obtained by summing up all the wheat production by

Table 3
Crop cultivar coefficients for CROPSIM and NWheat DDSAT V4.6.

CROPSIM								
Mega- environment[a]	Benchmark variety	VREQ[b]	PPS1[c]	P8[d]	G#WTS[e]	GWTS[f]	SHWTS[g]	PHINT[h]
Spring varieties								
1	SeriM82	20.0	40	490	22	40	1	120
1	PBW343	20.5	50	490	22	40	1	120
2A	Kubsa	20.5	50	490	22	40	1	120
2B	Tajan	20.5	50	490	22	40	1	120
4A	Bacanora (Kauz)	20.5	50	490	24	40	1	120
4B	DonErnesto	20.5	50	490	24	40	1	120
4C	HI 617 (Sujjatta)	21.0	50	490	24	40	1	120
Winter varieties								
12	Gerek79	27.0	105	430	22	45	1	135
N-Wheat								
Mega Environment	Benchmark variety	VSEN[i]	PPSEN[j]	P5[k]	GRNO[l]	MXFIL[m]	STMMX[n]	PHINT[o]
Spring varieties								
1	SeriM82	1.0	1.2	660	24	2	3	120
1	PBW343	1.2	1.5	660	24	2	3	120
2A	Kubsa	1.2	1.5	660	24	2	3	120
2B	Tajan	1.2	1.5	660	24	2	3	120
4A	Bacanora (Kauz)	1.2	1.5	660	26	2	3	120
4B	DonErnesto	1.2	1.5	660	26	2	3	120
4C	HI 617 (Sujjatta)	1.5	1.5	660	26	2	3	120
Winter varieties								
12	Gerek79	5.0	3.2	520	24	2.5	3	135

[a] Revised cultivar selection from Gbegbelegbe et al. (2017).
CROPSIM: [b] VREQ: Vernalization required for maximum development rate (days); [c] PPS1: Photoperiod sensitivity (% reduction in rate per 10 h drop in photoperiod phase); [d] P8: Grain filling period (degree days); [e] G#WTS: Standard grain number per unit canopy weight at anthesis (# g^{-1}); [f] GWTS: Standard grain size in optimum conditions, normal plant density (mg); [g] SHWTS: Standard, non-stressed shoot dry weight at maturity (including grain, g); [h] PHINT: Interval between successive leaf appearances (degree days).
NWheat: [i] VSEN: Sensitivity to vernalization; *j* PPSEN: Sensitivity to photoperiod; [k] P5: Thermal time (base 0°C) from beginning of grain filling to maturity; [l]GRNO: Coefficient of kernel number per stem weight at the beginning of grain filling (kernels g^{-1} stem); [m] MXFIL: Potential kernel growth rate (mg $kernel^{-1}$ per day); [n] STMMX: Potential final dry weight of a single tiller (excluding grain) (g $stem^{-1}$); [o] PHINT: Interval between successive leaf appearances (degree days).

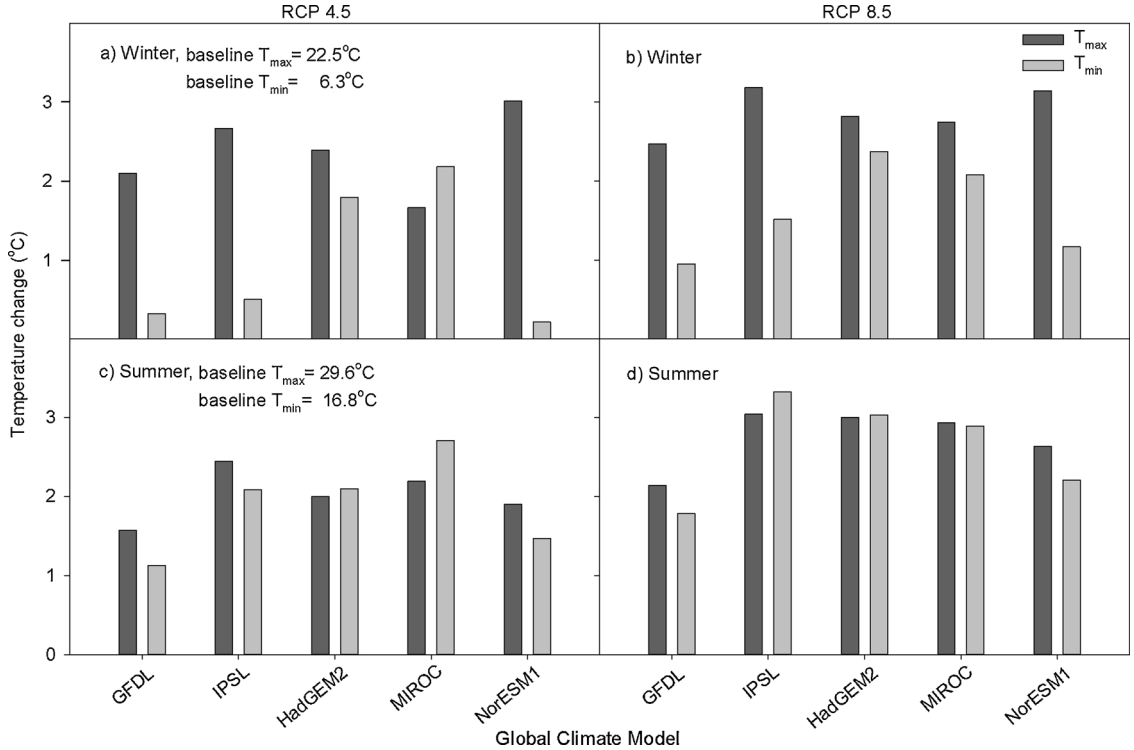

Fig. 2. Projected average maximum and minimum temperature change (to baseline, 1980–2010) for a and b) winter (December 10 to March 30) and c) and d) summer seasons (July 1 to Sept 7); for a) and, c), Representative Concentration Pathways 4.5 and b) and d) RPC 8.5, for the 2050s, Mexico, for five GCMs (Table 2).

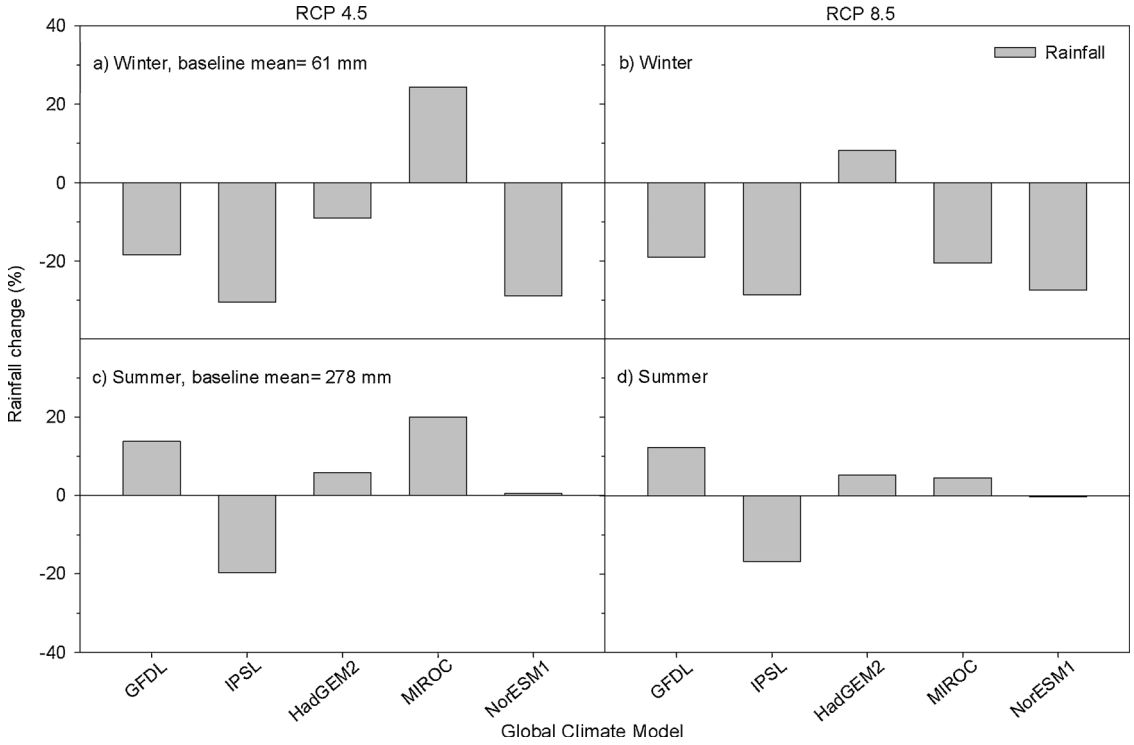

Fig. 3. Projected average rainfall change (to baseline, 1980–2010) for a) and b) winter (December 10 to March 30) and c) and d) summer seasons (July 1 to Sept 7); for a) and, c), Representative Concentration Pathways 4.5 and b) and d) RPC 8.5, for the 2050s, Mexico, for five GCMs (Table 2).

grid cell for the baseline and each RCP. Delta change of the RCPs relative to baseline period was then calculated by difference between RCP and baseline period.

2.5. Model uncertainty

Combined model uncertainty from the GCMs and crop simulation models from the point simulations was calculated and expressed as the 10^{th} and 90^{th} percentiles of the average of the 30 years for the 32 reference locations. Whereas for the spatial simulations, the 30-year average changes were calculated for each grid cell, and combined crop and GCM model uncertainty was calculated by taking the 10^{th} and 90^{th} percentiles of the grid cell value distribution.

3. Results

3.1. Climate

Temperature and rainfall for the baseline (1980–2010) showed spatial variation during winter and summer, with summer showing warmer temperatures and higher rainfall for most locations. The average temperature during the winter was 14.3 °C with seasonal rainfall averaging 61 mm (Table 1). Winter rainfall in the Northern area of Baja California was the highest, due to its Mediterranean-type climate, averaging 200 mm. The summer season was warmer with a 23.0 °C average temperature, and rainfall averaged 315 mm during the season (Table 1). Climate change scenarios show different magnitudes of temperature and rainfall changes for the 2050s in Mexico. However, all GCMs and both RCPs projected warmer temperatures with a steeper warming trend during the summer (Fig. 2). Maximum temperature (T_{max}) in both seasons tends to increase faster than the minimum temperature (T_{min}) (Fig. 2), which is the opposite to the global temperature trend (Solomon et al., 2007). Projected average warming during the winter for RCP 4.5 was 2.4 °C for T_{max} and 1.0 °C for T_{min}. For RCP 8.5, the temperature increase was higher, averaging 2.9 °C for T_{max} and 1.6 °C for T_{min} (Fig. 2a, b). Winter warming was higher in cooler locations in the north than in the southern states (data not shown). Summer temperatures were projected to increase by 2.0 °C for T_{max} and 1.9 °C for T_{min} for RCP 4.5, and by 2.7 °C and 2.6 °C for T_{max} and T_{min}, respectively, for RCP 8.5 (Fig. 2c, d). Rainfall projections showed large variability, with winter rainfall projected to decline by an average of 12.5% and 17.5% for RCP 4.5 and 8.5, respectively (Fig. 3a, b). Whereas summer rainfall projections ranged from a 5.9% increase to a 19.7% decrease, with similar variability under RCP 8.5 (Fig. 3c, d).

3.2. Model performance

Root mean square error (RMSE) for irrigated wheat was between 348 and 485 kg ha^{-1} and between 542 and 909 kg ha^{-1} for rainfed wheat (Fig. 4). Rainfed wheat showed higher RMSE, mostly caused by the model sensitivity to initial water conditions. Correlation coefficient for combined irrigated and rainfed wheat was highly significant ($P < 0.01$) with an $r^2 > 0.9$. Correlation coefficient for combined irrigated and rainfed wheat for the three major wheat producing states for irrigated and rainfed wheat was highly significant ($P < 0.01$) with an $r^2 > 0.90$. However, when conducting the individual analysis by state, correlations were low. Individual correlation coefficients for the major production states for irrigated wheat ranged between 0.2 and 0.03 while rainfed wheat showed even smaller coefficients, which were often not significant. Observed data used for this analysis was reported farmer data summarized per state, which combines a wide range of crop production practices (e.g. change between years and within a region in irrigation, fertilizer, sowing dates, cultivars, pest and disease, etc.) and yield levels across the state, while the simulated yields were point specific. Therefore, differences between simulated versus observed yield data are expected, causing a low correlation. The RMSE showed reasonable results indicating that the models represent the observed yield levels.

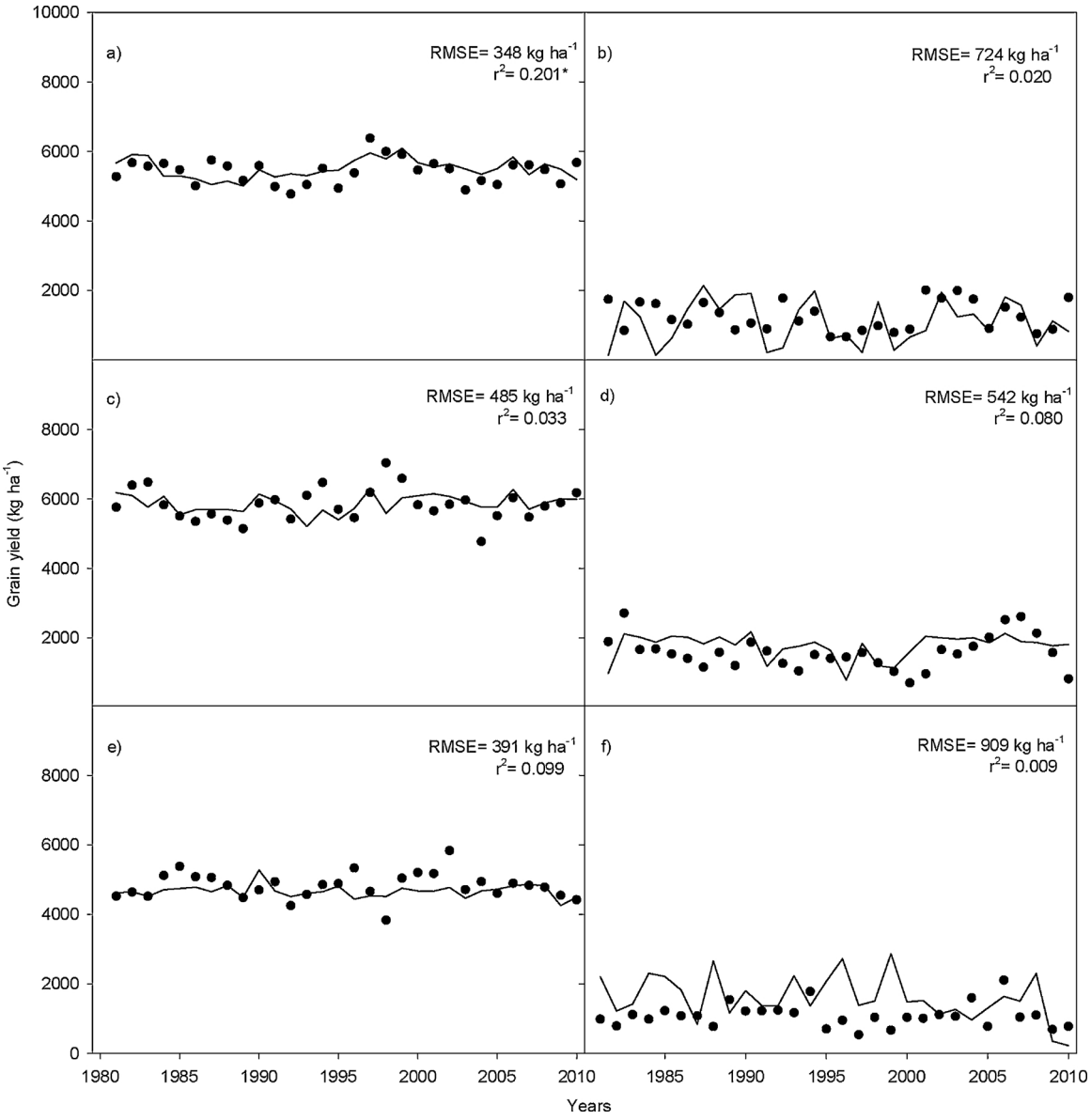

Fig. 4. Observed (symbol) and simulated (line) wheat grain yields, irrigated for a) Sonora (140 kg N ha^{-1}), c) Baja California (130 kg N ha^{-1}), e) Guanajuato (90 kg N ha^{-1}) and rainfed for b) Nuevo Leon (10 kg N ha^{-1}), d) Zacatecas (10 kg N ha^{-1}), and f) Guanajuato (10 kg N ha^{-1}) for the baseline period in Mexico (1980–2010) from SAGARPA (2016a). Observed wheat yields were detrended for technological improvements and adjusted to 0% grain moisture. Simulated wheat yields are the average of the CROPSIM and NWheat crop simulation models representing a state. Correlation analysis at 95% confidence interval for observed vs simulated wheat yields (combined irrigated and rainfed) for the three major wheat producing states in Mexico: $P < 0.01$, $r^2 = 0.91$. Significance at $P \leq 0.05$ level is indicated by *.

3.3. Climate change impact on Mexico wheat phenology and yields

3.3.1. Phenology

Simulated climate change impacts resulted in accelerated wheat phenology, with earlier flowering and a reduced grain filling period (time from anthesis to physiological maturity), during both seasons, as result of the warming temperatures under future scenarios (Fig. 2). The winter anthesis date for the baseline was in mid-March and was 6 days earlier for RCP 4.5 and 8 days earlier for RCP 8.5. The grain filling period was also affected, decreasing from 44 days in the baseline to 42 days under both RCPs. The anthesis date for summer-sown wheat was in early September for the baseline, but it was 4 days earlier for RCP 4.5 and 5 days earlier for RCP 8.5. The grain filling period for summer sown wheat was 5 and 7 days shorter in RCP 4.5 and 8.5, respectively.

3.3.2. Grain yields

Irrigated and rainfed wheat simulations suggest yield declines for most locations in Mexico by the 2050s due to projected warmer temperatures and decreased rainfall, despite the alleviating effect of CO_2. Fig. 5 shows relative yield change by GCM for irrigated and rainfed wheat for the 2050s in Mexico. Simulated irrigated wheat shows consistent yield declines for all GCMs in both RCPs with more pronounced declines for RCP 8.5. GFDL was the most optimistic GCM in both RCPs, as it projected the lowest temperature warming (Fig. 2). The highest temperature increase was projected in HadGEM2 for both RCPs, which resulted in the most pessimistic yield declines (Fig. 5a). Simulated rainfed wheat yield impacts are highly variable due to the combined effect of projected temperature and rainfall changes, suggesting mostly negative impacts, but ranging from a 44.3% yield increase to a 54.7% yield decrease for RCP 4.5 (Fig. 5b). Similar variability was observed in RCP 8.5, though simulated impacts tended to be ameliorated by the

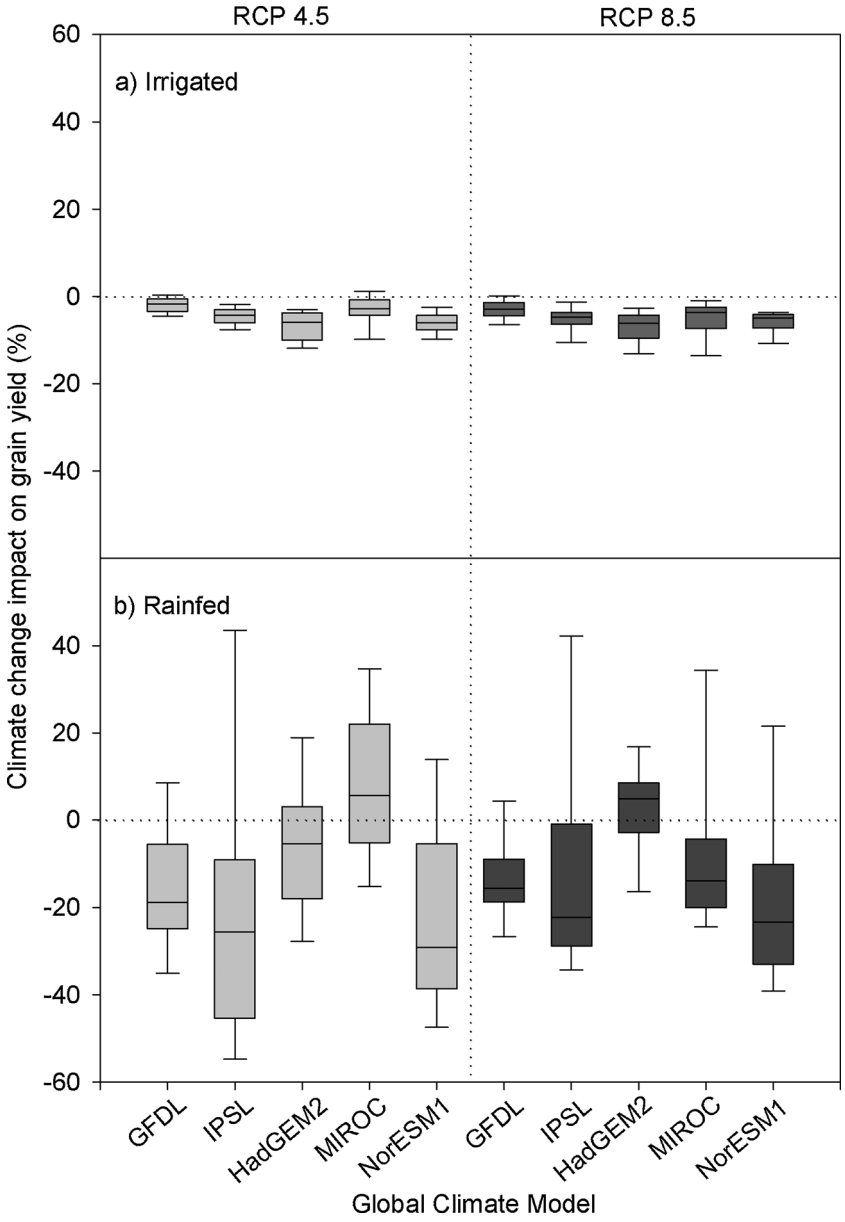

Fig. 5. Simulated climate change impact (including changes in temperature, rainfall, and atmospheric CO_2 concentration) on wheat yield in Mexico for a) irrigated and b) rainfed cropping systems, for five GCMs (Table 2) and two Representative Concentration Pathways (RCP 4.5 and 8.5) for 2050s. In each box plot, horizontal lines represent, from top to bottom, the 10th percentile, 25th percentile, median, 75th percentile and 90th percentile of the average of the 30 years, and two crop simulation models (CROPSIM and NWheat) for the 32 locations (Table 1).

alleviating effect of elevated CO_2 (Fig. 5b). Both crop simulation models captured similar responses to climate change by the 2050s (Fig. 6a). CROPSIM was more optimistic, projecting, in average, a negative climate change impact of $< -2.1\%$ in irrigated wheat yields for both RCPs. Whereas the NWheat model showed irrigated wheat yield declines for all locations, averaging -7.3% in RCP 4.5 and -8.3% in RCP 8.5 (Fig. 6a). With regards to simulated changes in rainfed wheat yields, both crop simulation models agreed, showing mostly negative impacts with large spatial variability, due to large variability in future climate scenarios (Fig. 6b). When averaging both models, climate change resulted in consistent negative impacts for irrigated and rainfed wheat production by the 2050s (Fig. 6a).

The crop models differed structurally on how they captured the temperature effects on wheat growth and yields by 2050, with NWheat showing more pessimistic impacts for both RCPs (Fig. 7a). In average, the crop models suggested negative yield effects on irrigated wheat as temperatures increased, showing -10.4% and -13.4% yield declines for RCP 4.5 and RCP 8.5, respectively (Fig. 7a). Average temperature impacts showed consistent irrigated wheat yield declines that are similar to reported observations from Ottman et al., (2012).

With regards to rainfed wheat, temperature and water stress impacts were larger and more variable due to already warm temperatures during summer, but also due to the added effect of spatial rainfall variability. The crop models tended to be more conservative when simulating the temperature impact on rainfed yields as compared to observations from Ottman et al., (2012), considering that future simulated rainfed yields also accounted for changes in rainfall. Simulations and observations show larger wheat yield declines per degree of temperature increase in already warm environments than in the cooler ones (Fig. 7).

In terms of CO_2 response, both models simulated on average positive CO_2 response for irrigated wheat yields in Mexico by the 2050s. Simulated irrigated wheat CO_2 response averaged 5.7% in RCP 4.5 and 8.0% in RCP 8.5, which is within the ranges reported in literature

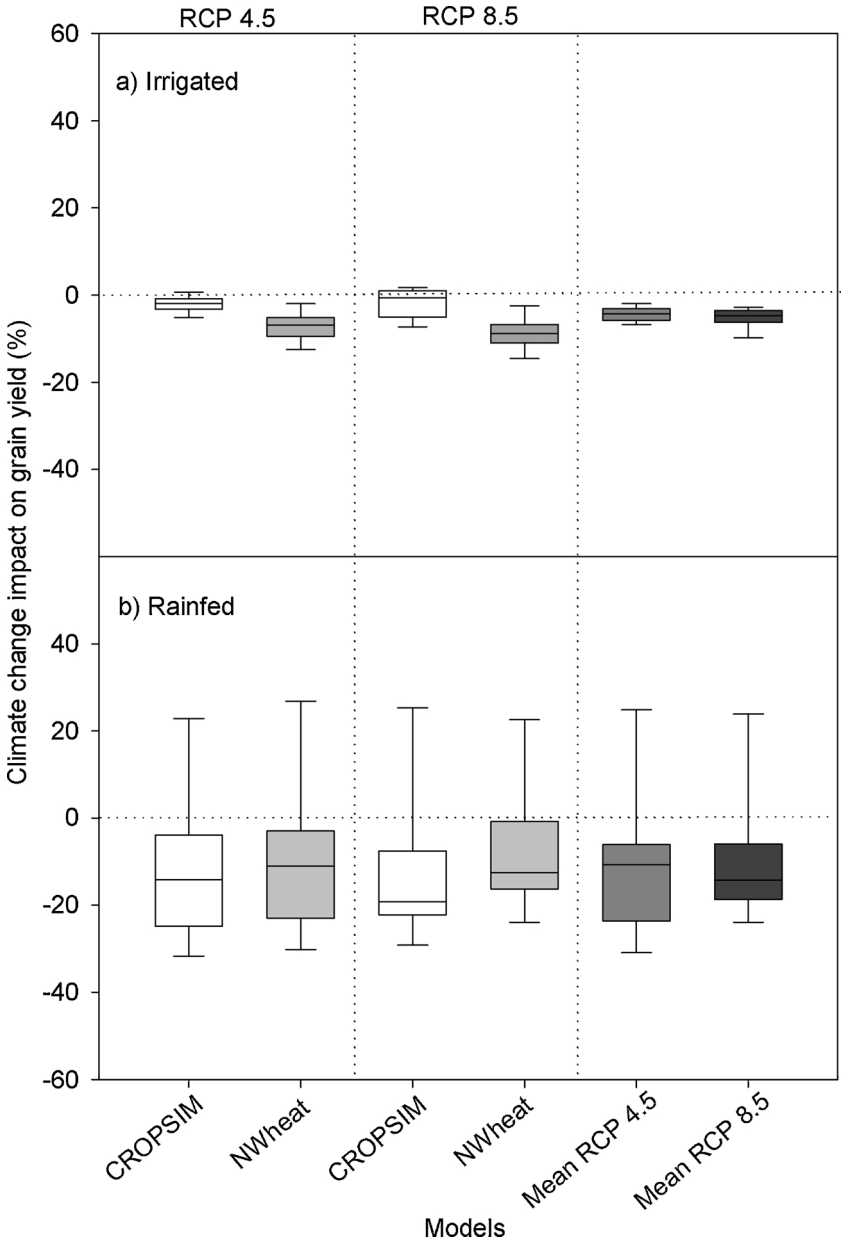

Fig. 6. Simulated climate change impact (including changes in temperature, rainfall, and atmospheric CO_2 concentration) on wheat yield in Mexico for a) irrigated and b) rainfed cropping systems, for two crop simulation models and two Representative Concentration Pathways (RCP 4.5 and 8.5) for 2050s. In each box plot, horizontal lines represent, from top to bottom, the 10th percentile, 25th percentile, median, 75th percentile and 90th percentile of the average of 30 years and five GCMs (Table 2) for the 32 locations (Table 1).

(Fig. 8a). The CO_2 response in rainfed wheat was lower, averaging 4.2 and 6.4% in RCP 4.5 and 8.5, respectively. The CO_2 response functions in both crop models are similar: The CROPSIM model simulates CO_2 response as a linear response, with positive biomass growth stimulus as atmospheric CO_2 increases above 330 ppm (base atmospheric CO_2 level), reaching the maximum response (43%) at 990 ppm atmospheric CO_2. With regards to NWheat, the CO_2 response is also linked to temperature, thus CO_2 response further increases with higher temperature to a maximum of 18 °C mean temperature, resulting in slightly higher CO_2 response than the CROPISM model (Asseng et al., 2004). Research also suggests that CO_2 effects can be larger under limited water, but high N supply (Fig. 8b). While CO_2 response tends to be mostly positive, few locations showed negative yield changes due to N stress limiting the positive effects of the CO_2.

Fig. 9 shows simulated irrigated and rainfed wheat yield changes by location for 2050. Simulated climate change impacts tend to be more consistent for irrigated wheat yields, while climate change impacts on rainfed yields were highly variable mostly due to rainfall spatial variability across Mexico. Irrigated wheat yields are suggested to decline up to -13% under RCP 4.5, except for North Zacatecas, where the warmer temperatures and elevated CO_2 improve suboptimal growing conditions. Locations in North Coahuila show the most negative impact of climate change due to already warm conditions during grain filling caused by late anthesis compared to the rest of the locations (data not shown). For RCP 8.5, simulated irrigated wheat yield changes tend to be more pessimistic with the majority of locations showing yield declines except for North Zacatecas, yet the positive effect there is still lower than for RCP 4.5 (Fig. 9a, b). The Northwestern states, where more than 75% of the irrigated wheat is currently grown are suggested to be one of the most affected regions in Mexico, as projected warming trends in this region are higher than in the southern states (Fig. 9a, b). Climate change impacts on rainfed wheat yields were larger showing

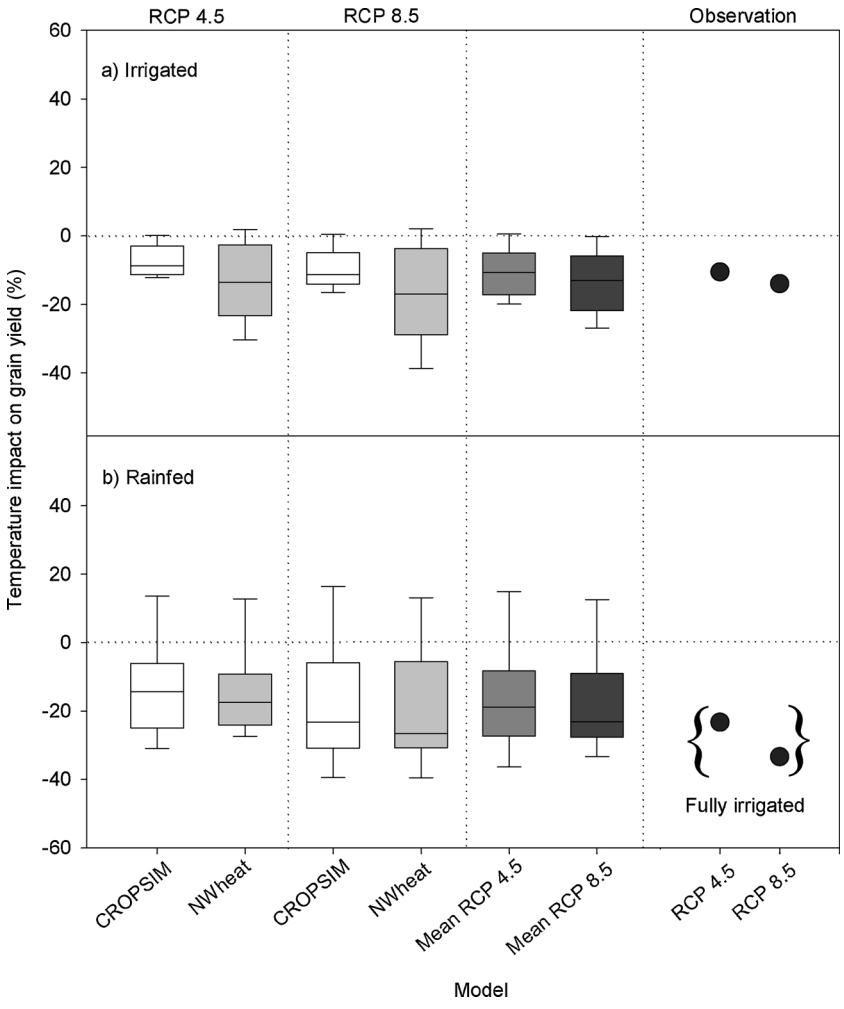

Fig. 7. Simulated temperature impact on wheat yield in Mexico a) irrigated and b) rainfed cropping systems, for two crop simulation models (CROPSIM and NWheat) and two Representative Concentration Pathways (RCP 4.5 and 8.5) for 2050s. In each box plot, horizontal lines represent, from top to bottom, the 10th percentile, 25th percentile, median, 75th percentile and 90th percentile of the average of 30 years and five GCMs (Table 2) for the 32 representative locations (Table 1). Future temperature effect corresponds to the simulated yield change for baseline atmospheric CO_2 concentration (362 ppm). Observations are based on measured temperature impacts for same background temperature and projected temperature change, derived from Ottman et al., (2012). Mean baseline temperature (winter = 15.1 °C, summer = 21.1 °C) and projected mean temperature change for RCP 4.5 (winter = + 1.8 °C, summer = + 1.6 °C) and RCP 8.5 (winter = + 2.4 °C, summer = + 2.3 °C) for Mexico.

mostly yield declines. However, important rainfed producing locations in Zacatecas, Michoacán, Oaxaca, and Chiapas show positive yield changes as a result of the improvement of suboptimal conditions either for temperature, rainfall or both but also due to the future elevated CO_2. The most negative impacts were observed in the Northwest, but rainfed production in this area is negligible. Yield declines tended to be higher for RCP 8.5 due to warmer temperature and a drier climate under this emission scenario. Spatial simulation method resulted in similar results of climate changes impacts on irrigated and rainfed wheat yields, showing similar variabilities between both methods; however, spatial simulations indicated slightly more negative impact than the point simulations (Fig. 10).

When weighting simulated wheat yield changes to observed district production and averaging for both methods, climate change impacts suggest a decline in aggregated (irrigated + rainfed) wheat production by 2050, with RCP 4.5 showing a yield impact of -5.0% and RCP 8.5 an impact of -5.9% (Fig. 11). Year to year variability is considerably smaller than spatial variability due to regional climate differences across Mexico. Model uncertainty tends to be large, mostly as result of the different magnitudes of climate change impacts captured by the crop simulation models, ranging from -0.7 to -13.6% for RCP 4.5 and from 2.2 to -15.4% for RCP 8.5. Upscaled climate change impact for the spatial simulation method showed slightly more negative impacts, with -8.9% for RCP 4.5 and -9.9% for RCP 8.5. Grid cell variability was larger than model uncertainty, as observed in the point simulations. However, model uncertainty for the spatial simulations was smaller than the point simulations.

4. Discussion

A multi-model ensemble allowed us to explore the effects of climate change on wheat yields by the 2050s, indicating negative climate change impacts on wheat production in Mexico. While previous studies in Mexico have attempted to determine the effects of climate change using either a limited number of GCMs and/or crop models or just exploring the sole effect of warming temperatures on wheat yields, in this study we explored the combined future effects of temperature, rainfall changes, and elevated CO_2 on wheat production using 5 GCMs and two-model ensembles with two scaling methods and quantified uncertainties. Spatial variability was larger than temporal variability, with most locations projecting yield declines, especially due to warming temperatures, and despite the alleviating effect of elevated atmospheric CO_2. Uncertainties were large, mostly as a result of structural differences in the crop simulation models, though when using the average of the two models, simulated yield responses were closer to observations than when comparing to a single model, like in previous studies (Asseng et al., 2014; Martre et al., 2015; Palosuo et al., 2011).

Previous studies also showed a wide range of climate responses, partly due to the use of a single GCM to conduct the studies and crop model assumptions and methods. Simulated climate change effects in our study show more conservative yield declines to the ones reported by SAGARPA and FAO (2012), who used one GCM (MIROC 3.2-HIRES) using one climate change scenario, A1B (IPCC, 2007), and a Ricardian method (Gbetibouo and Hassan, 2005; Mendelsohn and Dinar, 1999) to quantify yield changes in the future for the 2050s. Results from SAGARPA and FAO (2012) showed yield declines for South Sonora,

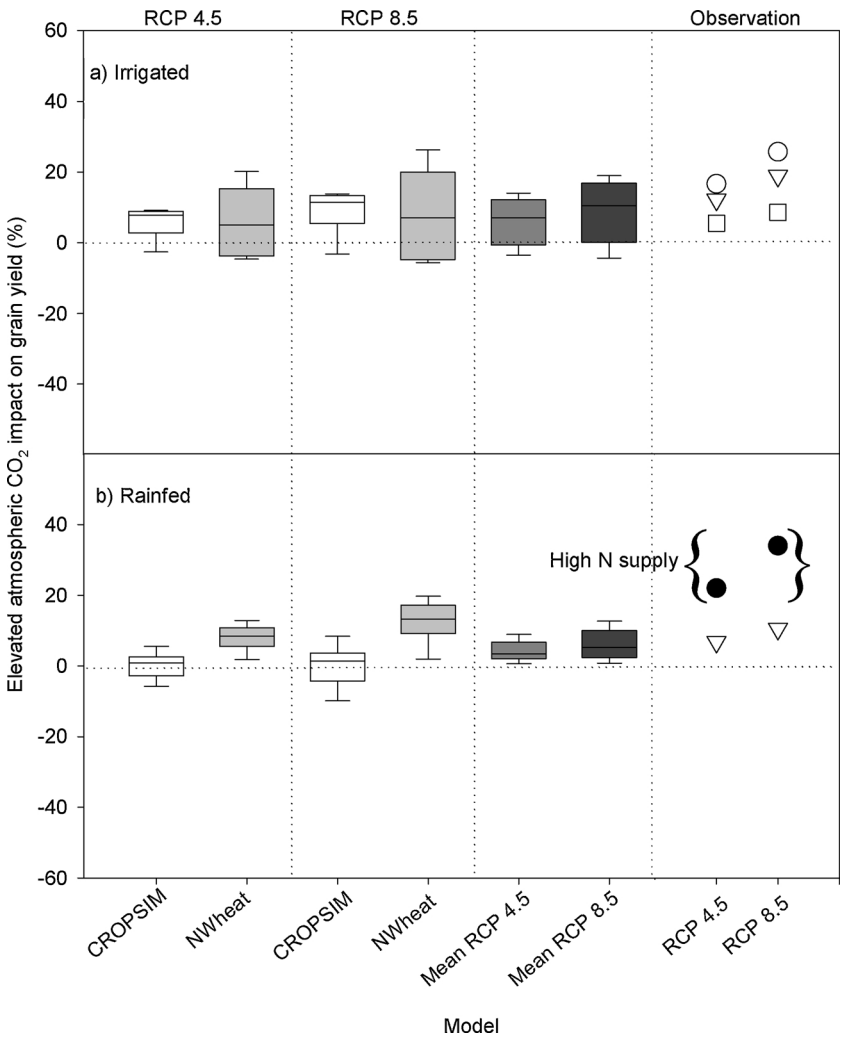

Fig. 8. Simulated elevated atmospheric CO_2 concentration impact on wheat yield in Mexico for a) irrigated and b) rainfed cropping systems, for two Representative Concentration Pathways (RCP 4.5 and 8.5) for 2050s. In each box plot, horizontal lines represent, from top to bottom, the 10th percentile, 25th percentile, median, 75th percentile and 90th percentile of the average of 30 years and five GCMs (Table 2) for the 32 locations (Table 1). Future CO_2 effect corresponds the difference between elevated atmospheric CO_2 concentration (RCP 4.5 = 498 ppm and RCP 8.5 = 572 ppm) vs baseline CO_2 (362 ppm). Observations were derived from measurements in field experiments with elevated atmospheric CO_2 adjusted to projected CO_2 concentrations, based on O'Leary et al. (2015) (circles), Kimball et al. (2001) (triangles) and Kimball et al. (1995) (squares).

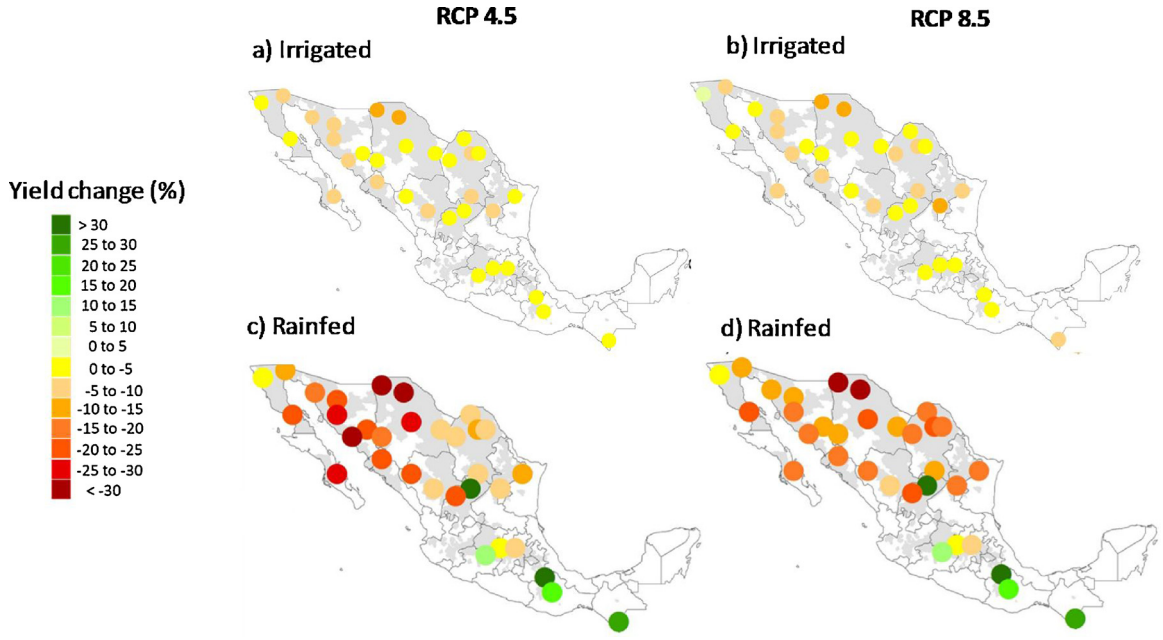

Fig. 9. Simulated climate change impact (including changes in temperature, rainfall and atmospheric CO_2 concentration) on wheat yield in Mexico for a and b) irrigated and c and d) rainfed systems for a and c) Representative Concentration Pathways 4.5 and b and d) 8.5, for 2050s. Impacts represent the average of 30 years, two crop simulation models (CROPSIM and NWheat) and five GCMs (Table 2).

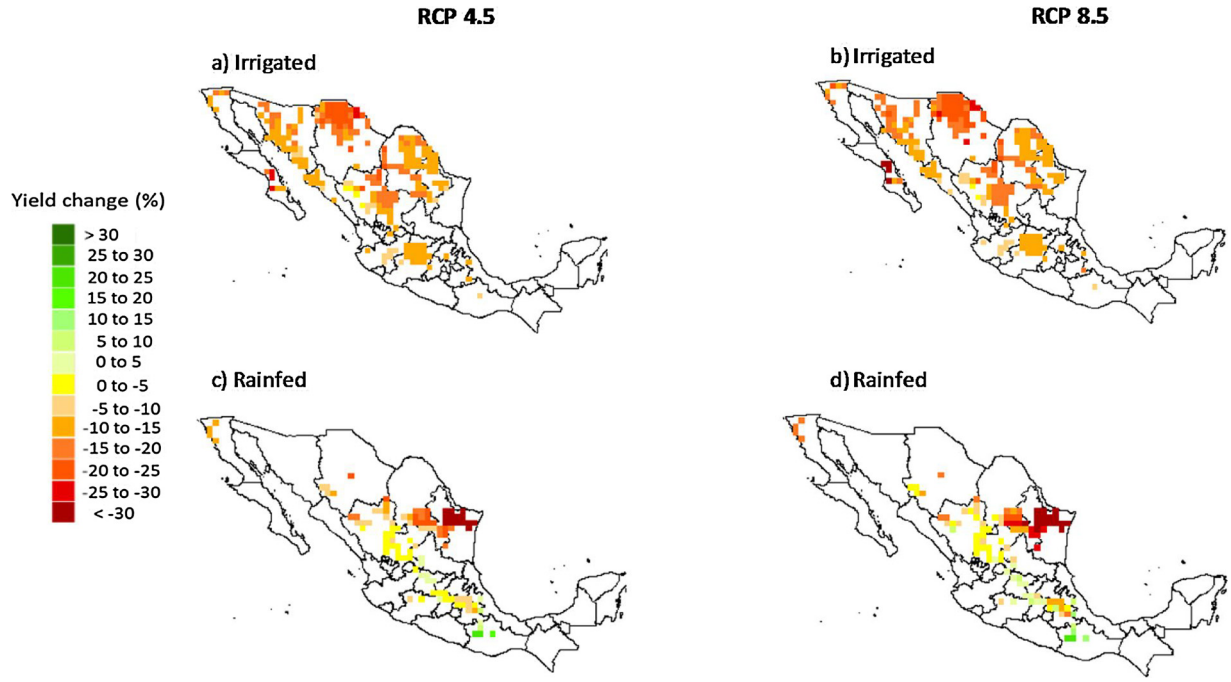

Fig. 10. Simulated climate change impact (including changes in temperature, rainfall and atmospheric CO_2 concentration) on wheat yield in Mexico for a and b) irrigated and c and d) rainfed systems for a and c) Representative Concentration Pathways 4.5 and b and d) 8.5, for 2050s. Impacts represent the average of 30 years, two crop simulation models (CROPSIM and NWheat) and five GCMs (Table 2). Gridded simulations using the DSSAT software linked to the MINK system (Robertson, 2017).

South Baja California, and North Sinaloa ranging from 25 to 75% as result of changes in temperature and precipitation. By contrast, they reported yield increases in Baja California and North Sonora by up to 50%. Our results are very different to SAGARPA and FAO (2012), but more similar to the ones reported by Parry et al. (2004), who used the climate change SRES scenarios from the IPCC (2001) report (IPCC, 2001) and yield transfer functions to estimate yield impacts. This particular study, however, was conducted using only one GCM (HadGEM3), where the projected temperature increase ranged from 1 to 2 °C and elevated CO_2 ranged from 460 to 500 ppm for mid-century. Cereal yield decline at the national level ranged from 5 to 10%, even when applying adaptation strategies such as changes in sowing dates, fertilizer, and irrigation management. Climate change responses for the previously discussed studies showed large uncertainties, because GCMs tend to vary widely on climate projections, in addition to the uncertainty caused by using only one technique to estimate yield impacts.

Warm temperatures cause accelerated plant phenology, shortening the growth cycle as degree days accumulate faster. Under warm temperatures, the number of spikelets and the number of kernels per spikelet decrease, resulting in reduced grain number (Johnson and Kanemasu, 1983). Heat stress caused by temperatures above 32 °C after anthesis accelerate leaf senescence (Al-khatib and Paulsen, 1984), and the grain filling period tends to be shorter, limiting time for grain growth (Asseng et al., 2014). The crop simulation models used in the current study were able to capture the effects of temperature, simulating earlier anthesis, reduced grain filling period, and reduced yields under projected warmer temperatures. Our study suggests consistent irrigated wheat yield declines of 6.2% per degree temperature increase during the winter, which is within reported ranges. Rainfed wheat systems showed larger and more variable responses than irrigated systems, because of the combined effects of already warm baseline temperatures (Liu et al., 2016) and future rainfall declines, with projected yield reductions ranging from 5.0 to 7.0% per degree increase in temperature during the summer. Sayre et al. (1997) reported that increases by 1.0 °C during the period from January to April in Sonora, Mexico resulted in anthesis occurring 11 days earlier, and the grain filling period being shortened by 3 days, which is similar to our simulated phenology; grain yields declined by 8.5% on average over the 6-year studied period. Asseng et al. (2014) reported a 6% yield decline per degree of global warming, but also found that simulated yield losses were larger in already warm regions. Lobell et al. (2011) reported a 5.5% yield decline per degree of global warming using statistical methods. In a recent study conducted in Sudan, which is a temperature hotspot location, yield decline per degree of warming was estimated at 5.9% for a 13 °C baseline temperature, yield declines are much higher in locations where temperatures reached 27 °C (Asseng et al., 2017). O'Leary et al., 2015showed that irrigated wheat yield declined as temperature increased and that temperature impacts were larger at warmer temperatures than at cooler temperatures (Fig. 7). A similar trend was observed by Liu et al. (2016), who suggested that warmer locations in the world tended to have more negative effects as temperatures increased. By contrast, in another study, Lobell et al. (2005) suggested that yield increase over the period from 1980 to 2001 was mostly due to cooling trends in night temperatures benefiting plant growth. In our study, a few exceptions occurred where climate change improved suboptimal growing conditions. Simulated irrigated yields for North Zacatecas showed a positive yield response due to improvements on suboptimal temperature and CO_2 conditions. In the case of rainfed wheat locations in the south with > 500 mm precipitation, yields are actually benefited by small declines in rainfall, as the crop can take better advantage of the applied N due to less leaching occurring under the projected climate scenarios.

Irrigated systems were simulated using automatic irrigation, therefore, water stress was minimal, although it has been reported that water stress effects tend to be more severe as temperature increases (Shah and Paulsen, 2003). In the case of rainfed wheat, supplemental irrigation may be an option to reduce the negative effects of rainfall variability (Xiao et al., 2005), and as a result to decrease water stress and increase yields, which in turn may help to reduce future climate change effects.

Differences in CO_2 response were due to structural differences in how the models simulate the CO_2 effects on biomass accumulation. However, crop models do well at reproducing FACE experiment data,

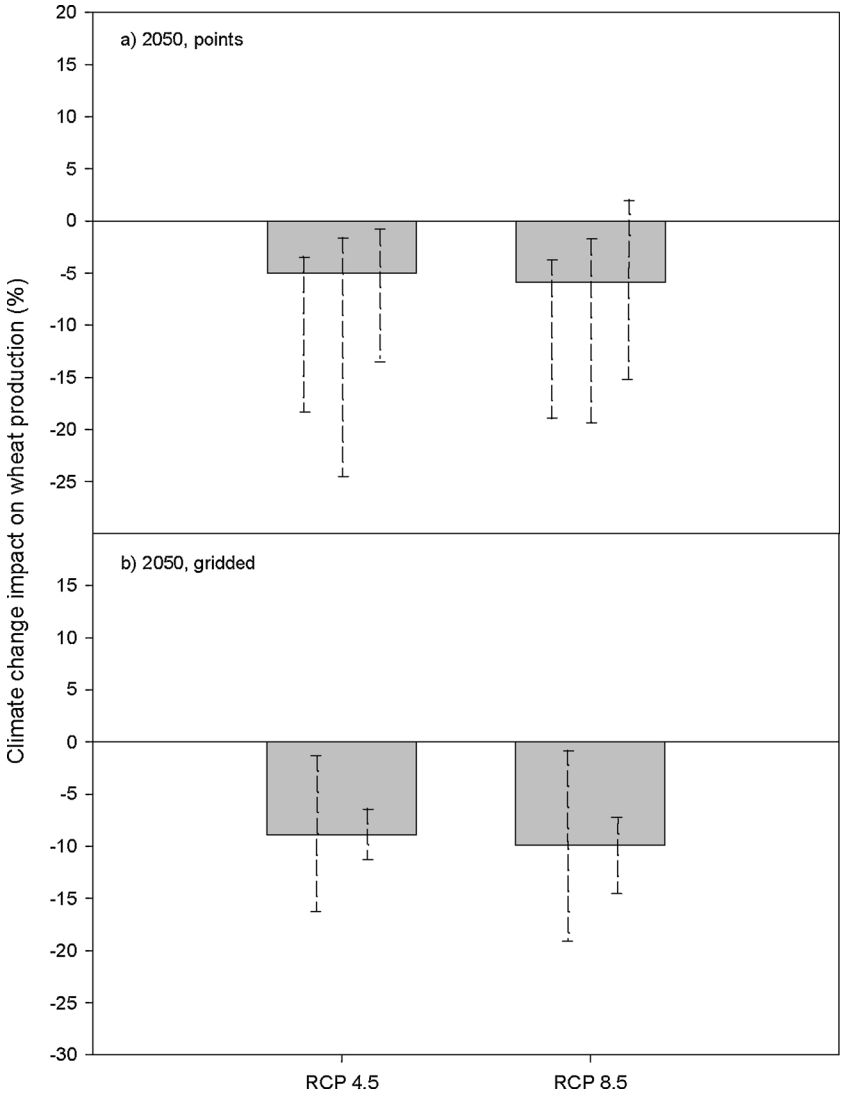

Fig. 11. a) Simulated climate change impact (including changes in temperature, rainfall, and atmospheric CO_2 concentration) on wheat yield in Mexico (upscaled via district reported production in 2015 represented by each simulated location) and b) aggregated from grid cells for two Representative Concentration Pathways (RCP 4.5 and 8.5), for 2050s. Error bars (from top to bottom indicating 10^{th} and 90^{th} percentile) from the left to right represent variability of 30 years, variability of 32 locations in (a) or variability of grid cells in (b), and uncertainty from models (combined two crop simulation models - CROPSIM and NWheat, and five GCMs (Table1 and 2).

which gives us confidence in our results (Asseng et al., 2014, 2004; O'Leary et al., 2015). Crop model response to CO_2 is also related to N availability. CO_2 response is lower in the presence of N stress, suggesting that increased N fertilizer use may be an adaptation strategy to improve crop yields in the future, which has been suggested in previous studies (Kimball, 2016; Kimball et al., 2001). FACE experiments also show that under water stress, but high N supply, the CO_2 response tends to be even larger than under adequate growing conditions (Kimball et al., 2001, 1995).

Despite the differences in model initialization and the simulation process per se (points vs spatial), both methods resulted in similar climate change impacts on wheat production by 2050. Liu et al. (2016) and Zhao et al. (2017) also showed that point and gridded simulation produce similar impacts in regional and global analysis for temperature impacts.

5. Limitations

5.1. Observed data

Yield comparisons to the baseline yields were conducted using state yield level data from SAGARPA (2016a) and indicated that simulated yields were within the range of reported yield data. However, simulated yield dynamics in the baseline differed from the observed data. Differences were possibly caused, in part, by different grower practices. In addition, generalizations in crop management practices and crop genetic coefficients may have introduced uncertainty to the simulated wheat yields, adding to the differences in simulated yields.

5.2. Crop management

Irrigated wheat simulations were conducted using one representative planting date for all reference locations, while two planting dates were used for rainfed areas. In reality, however, the planting window for the winter cycle is between mid-November to mid-December, and in locations like Sinaloa and Nuevo Leon the planting time window extends till the end of December. For rainfed wheat in the central region, the planting window is between mid-May and mid-June, when rainfall starts to occur.

With regards to fertilizer applications, N fertilizer was set to be region-specific based on the observed state wheat yields for the baseline. But in reality, fertilizer practices are not standardized, possibly leading to uncertainties concerning the role that elevated atmospheric CO_2 will play in the future, since crop response to elevated CO_2 is linked to N availability.

Large differences were also observed when comparing observed and simulated rainfed wheat yields, primarily resulting from crop model sensitivity to initial water conditions. Under the present study, initial water conditions were set to avoid crop losses due to water related germination restrictions built into the models. In reality, under rainfed

circumstances water accumulated in the soil profile previous to planting plays an important role in heavy soils, where the stored water helps to maintain the crop early on the season, even when rainfall may be minimal during this period.

5.3. Crop genetic coefficients

Crop genetic coefficients based on mega-environments were collected from Gbegbelegbe et al. (2017) and translated to the NWheat and CROPSIM model. Because calibration was carried with field data for the used cultivars, crop genetic coefficients may be adding to the uncertainty of the study. However, phenology for spring varieties, which were the most common type used, was compared to 6 years of observed data for spring cultivars and experts knowledge (Sayre et al., 1997), giving confidence in the used crop genetic coefficients.

5.4. Irrigation practices

Irrigated wheat simulations were conducted by using automatic irrigation to avoid water stress during the season. As temperature increases, however, crop water stress effects tend to be more negative. Therefore, it is likely that if the crop is subjected to higher water stress in the future than it currently is, larger negative climate change impacts may be expected.

6. Conclusions

Climate change impacts were quantified together with their uncertainties through the use of a crop-climate multimodel ensemble, an approach which provides a more comprehensive assessment than the ones conducted previously, where single models were used and lacked any quantification of uncertainty. Climate change poses a threat to one of the major cereal crops in Mexico with warming temperatures already causing yield declines in major production areas, such as Northwest Mexico. Climate change in the future is projected to exacerbate the effects of temperature, especially in the Northwest, regardless of the growth-stimulating effects of CO_2. Adaptation strategies such as introducing heat tolerant cultivars, early vigor, and changes in phenology may be the most feasible way to cope with the negative effects of climate change, in particularly temperature increase. Change in crop management, such as early planting or N application rates may also offer additional benefits. Expanding wheat cropping could be an option in some regions, however, water availability for irrigation might be limited. Future water availability for even current wheat cropping area is already an issue, since many aquifers are over-used or have conditions of saline water intrusion (CNA, 2016; Curiel, 2013). An integrated assessment of climate change adaptation strategies should be conducted considering the sustainability of these practices in terms of feasibility and practicability. Implementing adaptation measures in the future could assist to maintain and improve wheat production for the coming decades in Mexico.

Acknowledgements

The authors acknowledge financial support from: the International Maize and Wheat Improvement Center (CIMMYT), the Mexico's Ministry of Agriculture (Secretaria de Agricultura, Ganaderia, Desarrollo Rural, Pesca y Alimentación, SAGARPA) through the Sustainable Modernization of Traditional Agriculture (MasAgro) project, and the CGIAR Platform for Big Data in Agriculture. We thank Kirsten Paff for input to an earlier draft and the Agricultural Model Intercomparison and Improvement Project (AgMIP) for support.

References

Alexandrov, V.A., Hoogenboom, G., 2000. Vulnerability and adaptation assessments of agricultural crops under climate change in the Southeastern USA. Theor. Appl. Climatol. 67 (1-2), 45–63.
Al-khatib, K., Paulsen, G.M., 1984. Mode of high-temperature injury to wheat during grain development. Physiol. Plant. 61 (3), 363–368.
Asseng, S., 2004. Wheat Crop Systems: a Simulation Analysis. CSIRO Publishing, Melbourne, Australia 275 pp.
Asseng, S., Turner, N.C., 2007. Modelling genotype× environment× management interactions to improve yield, water use efficiency and grain protein in wheat. Frontis 21, 91–102.
Asseng, S., et al., 1998. Use of the APSIM wheat model to predict yield, drainage, and NO_3 leaching for a deep sand. Aust. J. Agric. Res. 49 (3), 363–377.
Asseng, S., van Keulen, H., Stol, W., 2000. Performance and application of the APSIM nwheat model in the Netherlands. Eur. J. Agron. 12, 37–54.
Asseng, S., Turner, N.C., Ray, J.D., Keating, B.A., 2002. A simulation analysis that predicts the influence of physiological traits on the potential yield of wheat. Eur. J. Agron. 17 (2), 123–141.
Asseng, S., et al., 2004. Simulated wheat growth affected by rising temperature, increased water deficit and elevated atmospheric CO_2. Field Crops Res. 85 (2–3), 85–102.
Asseng, S., et al., 2013a. Uncertainty in simulating wheat yields under climate change. Nat. Clim. Change 3 (9), 827–832.
Asseng, S., Royce, F., Cammarano, D., 2013b. Temperature routines in nwheat. Alderman, P., Quilligan, E., Asseng, S., Ewert, F., Reynolds, M. (Eds.), Proceedings of the Workshop: Modeling Wheat Response to High Temperature. CIMMYT, El Batan.
Asseng, S., et al., 2014. Rising temperatures reduce global wheat production. Nat. Clim. Change 5 (2), 143–147.
Asseng, S., et al., 2017. Hotspots of wheat yield decline with rising temperatures. Global Change Biol. 23, 2464–2472.
Challinor, A.J., et al., 2014. A meta-analysis of crop yield under climate change and adaptation. Nat. Clim. Change 4, 287–291.
CNA, 2016. Estadísticas del agua en México, Comision Nacional de Agua. Secretaria del Medio Ambiente y Recursos Naturales, Mexico City, Mexico.
Conde, C., Estrada, F., Martinez, B., Sanchez, O., Gay, C., 2011. Regional climate change scenarios for México. Atmosphera 24 (1), 125–140.
Curiel, R., 2013. MasAgro por la seguridad alimentaria y el desarrollo agrícola sustentable de México. Revista Claridades Agropecuarias 237, 9–18.
Curtis, B.C., 2002. Wheat in the world. In: Curtis, B.C., Rajaram, S., Gómez Macpherson, H. (Eds.), Bread Wheat. Publishing and Multimedia Service, Information Division, FAO, Rome, Italy pp. 554.
Dale, A., Fant, C., Strzepek, K., Lickley, M., Solomon, S., 2017. Climate model uncertainty in impact assessments for agriculture: a multi-ensemble case study on maize in sub-Saharan Africa. Earths Future 5 (3), 337–353.
Escobar, R., 2014. El cultivo de secano. Universidad Autónoma Chapingo, Texcoco, México.
Gbegbelegbe, S., et al., 2017. Baseline simulation for global wheat production with CIMMYT mega-environment specific cultivars. Field Crops Res. 202, 122–135.
Gbetibouo, G.A., Hassan, R.M., 2005. Measuring the economic impact of climate change on major South African field crops: a ricardian approach. Global Planet. Change 47 (2-4), 143–152.
Giorgi, F., Francisco, R., 2000. Evaluating uncertainties in the prediction of regional climate change. Geophys. Res. Lett. 27 (9), 1295–1298.
Guttman, N.B., 1989. Statistical descriptors of climate. Bull. Am. Meteorol. Soc. 70 (6), 602–607.
Hunt, L.A., Pararajasingham, S., 1995. CROPSIM-wheat - a model describing the growth and development of wheat. Can. J. Plant. Sci. 75 (3), 619–632.
IPCC, 2001. The scientific basis. Contribution of Working Group I to the Third Assessment Report of the Intergovernmental Panel on Climate Change. Cambridge University Press, Cambridge, United Kingdom and New York, NY, USA 881 pp.
IPCC, 2007. Intergovernmental panel on climate change), 2007 global climate projection. climate change 2007. In: Solomon, S., Qin, D., Manning, M., Chen, Z., Marquis, M., Averyt, K.B., Tignor, M., Miller, H.L. (Eds.), The Physical Science Basis. Contribution of Working Group I to the Fourth Assessment Report of the Intergovernmental Panel on Climate Change, pp. 749–844.
IPCC, 2013. Climate change 2013. The Physical Science Basis. Contribution of Working Group I to the Fifth Assessment Report of the Intergovernmental Panel on Climate Change. Cambridge, UK and New York, US.
Johnson, R.C., Kanemasu, E.T., 1983. Yield and development of winter wheat at elevated temperatures. Agron. J. 75 (3), 561–565.
Jones, J.W., et al., 2003. The DSSAT cropping system model. Eur. J. Agron. 18 (3-4), 235–265.
Kalnay, E., et al., 1996. The NCEP/NCAR 40-year reanalysis project. Bull. Am. Meteorol. Soc. 77 (3), 437–471.
Karmalkar, A.V., Bradley, R.S., Diaz, H.F., 2011. Climate change in Central America and Mexico: regional climate model validation and climate change projections. Clim. Dyn. 37 (3-4), 605–629.
Kassie, B.T., Asseng, A., Porter, C.H., Royce, F., 2016. Performance of DSSAT-nwheat across a wide range of current and future growing conditions. Field Crops Res.
Kimball, B.A., 2016. Crop responses to elevated CO_2 and interactions with H_2O, N, and temperature. Curr. Opin. Plant Biol. 31, 36–43.
Kimball, B.A., et al., 1995. Productivity and water use of wheat under free-air CO_2 enrichment. Global Change Biol. 1 (6), 429–442.
Kimball, B.A., et al., 2001. Elevated CO_2, drought and soil nitrogen effects on wheat grain quality. New Phytol. 150, 295–303.
Koo, J., Dimes, J., 2010. HC27: Generic/Prototypical Soil Profiles. Available online at. International Food Policy Research Institute, Washington, DC., and University of Minnesota, St. Paul, MN. http://harvestchoice.org/node/2239.
Kottek, M., Grieser, J., Beck, C., Rudolf, B., Rubel, F., 2006. World map of the koppen-

geiger climate classification updated. Meteorol. Z. 15 (3), 259–263.
Lazzaretti, A.T., Fernandes, J.M., Pavan, W., 2015. Calibration of cropsim-wheat in the development of wheat in southern Brazil. Revista Brasileira de Ciencias Agrarias (Agraria) 10 (3), 356–364.
Limon-Ortega, A., Villaseñor-Mir, E., 2006. Nitrogen fertilizer management and recommendations for wheat production in central Mexico. Crop Manage. 5, 10.
Liu, B., et al., 2016. Similar estimates of temperature impacts on global wheat yield by three independent methods. Nat. Clim. Change 6, 1130–1138.
Lobell, D.B., et al., 2005. Analysis of wheat yield and climatic trends in Mexico. Field Crops Res. 94 (2-3), 250–256.
Lobell, D.B., Schlenker, W., Costa-Roberts, J., 2011. Climate trends and global crop production since 1980. Science 333 (6042), 616–620.
Martre, P., et al., 2015. Multimodel ensembles of wheat growth: many models are better than one. Global Change Biol. 21 (2), 911–925.
Mendelsohn, R., Dinar, A., 1999. Climate change, agriculture, and developing countries: does adaptation matter? World Bank. Res. Observer 14 (2), 277–293.
Monfreda, C., Ramankutty, N., Foley, J., 2008. Farming the planet: 2. Geographic distribution of crop areas, yields, physiological types, and net primary production in the year 2000. Global Biogeochem. Cycles 22 (1), 19.
Mueller, C., Robertson, R.D., 2014. Projecting future crop productivity for global economic modeling. Agric. Econ. 45 (1), 37–50.
O'Leary, G.J., et al., 2015. Response of wheat growth, grain yield and water use to elevated CO_2 under a Free-air CO_2 enrichment (FACE) experiment and modelling in a semi-arid environment. Global Change Biol. 21 (7), 2670–2686.
Ottman, M.J., Kimball, B.A., White, J.W., Wall, G.W., 2012. Wheat growth response to increased temperature from varied planting dates and supplemental infrared heating. Agron. J. 104 (1), 7–16.
Palosuo, T., et al., 2011. Simulation of winter wheat yield and its variability in different climates of Europe: a comparison of eight crop growth models. Eur. J. Agron. 35 (3), 103–114.
Parry, M.L., Rosenzweig, C., Iglesias, A., Livermore, M., Fischer, G., 2004. Effects of climate change on global food production under SRES emissions and socio-economic scenarios. Global Environ. Change-Hum. Policy Dimens. 14 (1), 53–67.
Peterson, A.T., et al., 2002. Future projections for Mexican faunas under global climate change scenarios. Nature 416 (6881), 626–629.
Ramirez-Rodrigues, M.A., et al., 2016. The value of seasonal forecasts for irrigated, supplementary irrigated, and rainfed wheat cropping systems in northwest Mexico. Agric. Syst. 147, 76–86.
Robertson, R., 2017. Mink, Details of a Global Gridded Crop Modeling System. International Food Policy Research Institute, Washington DC, USA 261 pp.
Rosenzweig, C., et al., 2013. The agricultural model intercomparison and improvement project (AgMIP): protocols and pilot studies. Agric. For. Meteorol. 170, 166–182.
Rotter, R.P., et al., 2012. Simulation of spring barley yield in different climatic zones of Northern and Central Europe: a comparison of nine crop models. Field Crops Res. 133, 23–36.
Ruane, A., et al., 2016. Multi-wheat-model ensemble responses to interannual climate variability. Environ. Modell. Softw. 81, 86–101.
SAGARPA, 2016a. Anuario estadístico de la producción agrícola. Available at:. http://infosiap.siap.gob.mx/aagricola_siap_gb/icultivo/index.jsp.
SAGARPA, 2016b. Crece 19 por ciento rendimiento en produccion de trigo en Mexico. Secretaria de Agricultura, Ganaderia, Desarrollo Rural, Pesca y Alimentacion, Ciudad de Mexico, Mexico.
SAGARPA and FAO, 2012. Mexico: El sector agropecuario ante el desafío del cambio climático, Mexico City, Mexico.
Sayre, K.D., Rajaram, S., Fischer, R.A., 1997. Yield potential progress in short bread wheats in northwest Mexico. Crop Sci. 37 (1), 36–42.
Semenov, M.A., Stratonovitch, P., 2010. Use of multi-model ensembles from global climate models for assessment of climate change impacts. Climate Res. 41 (1), 1–14.
Shah, N.H., Paulsen, G.M., 2003. Interaction of drought and high temperature on photosynthesis and grain-filling of wheat. Plant. Soil. 257 (1), 219–226.
Solomon, S., et al., 2007. Climate Change 2007: the Physical Science Basis. Contribution of Working Group I to the Fourth Assessment Report of the Intergovernmental Panel on Climate Change. Summary for Policymakers. Climate Change 2007: the Physical Science Basis. Contribution of Working Group I to the Fourth Assessment Report of the Intergovernmental Panel on Climate Change. Summary for Policymakers 18 pp.
Tebaldi, C., Knutti, R., 2007. The use of the multi-model ensemble in probabilistic climate projections. Philosophical Transactions the Royal Society A - Mathematical Physical Engineering Sciences 365 (1857), 2053–2075.
van Bussel, L.G.J., et al., 2016. Spatial sampling of weather data for regional crop yield simulations. Agric. For. Meteorol. 220, 105–115.
Van Ittersum, M.K., Howden, S.M., Asseng, S., 2003. Sensitivity of productivity and deep drainage of wheat cropping systems in a Mediterranean environment to changes in CO_2, temperature and precipitation. Agric. Ecosyst. Environ. 97 (1), 255–273.
Wallach, D., Mearns, L.O., Ruane, A.C., Rötter, R.P., Asseng, S., 2016. Lessons from climate modeling on the design and use of ensembles for crop modeling. Clim. Change 139, 551–564.
WMO, 1989. Calculation of Monthly and Annual 30-Year Standard Normals (WCDP928 No.10, WMO-TD/No.341). World Meteorological Organization, Geneva.
Xiao, G., Liu, W., Xu, Q., Sun, Z., Wang, J., 2005. Effects of temperature increase and elevated CO2 concentration, with supplemental irrigation, on the yield of rain-fed spring wheat in a semiarid region of China. Agric. Water Manage. 74 (3), 243–255.
Yin, X., et al., 2017. Multi-model uncertainty analysis in predicting grain N for crop rotations in Europe. Eur. J. Agron. 84, 152–165.
Zadoks, J.C., Chang, T.T., Konzak, C.F., 1974. A decimal code for the growth stages of cereals. Weed Res. 14, 415–421.
Zhao, C., et al., 2017. Temperature increase reduces global yields of major crops in four independent estimates. Proceedings of the National Academy of Sciences of the United States of America 114 (35), 9326–9331.
Zheng, B., Chenu, K., Doherty, A., Chapman, S., 2015. The APSIM-wheat module (7.5 R3008). Agricultural Production Systems Simulator (APSIM) Initiative.